Innovative patterning method for modifying few-layer MoS2 device geometries

Fernando Jiménez Urbanos[1a], Andrés Black[a,b], Ramón Bernardo-Gavito[c], Manuel R. Osorio[a], Santiago Casado[a], Daniel Granados[a]

a. Fundación IMDEA Nanociencia, C/Faraday, 9, 28049, Madrid, Spain
b. Departamento de física de la materia condensada, Universidad Autónoma de Madrid, Cantoblanco, 28049, Madrid, Spain
c. Physics Department, Lancaster University, LA1 4YB, Lancaster, United Kingdom

ABSTRACT:

When mechanically exfoliated two-dimensional (2D) materials are used for device applications, their properties strongly depend on the geometry and number of layers present in the flake. In general, these properties cannot be modified once a device has been fabricated out of an exfoliated flake. In this work we present a novel nano-patterning method for 2D material based devices, Pulsed eBeam Gas Assisted Patterning (PEBGAP), that allows us to fine tune their geometry once the device fabrication steps have been completed.

1. INTRODUCTION:

Transition metal dichalcogenides (TMDCs) such as MoS_2, which are considered candidates for next generation optoelectronic technology, consist of discrete two-dimensional (2D) layers bound together by weak van der Waals forces. For that reason, flakes can be exfoliated easily by the Scotch-tape method [1]. These flakes exhibit distinctive thickness dependent variations in their physical properties [2-5].

The band structure of MoS_2 varies with the multilayer thickness, going from a direct bandgap in single layer (SL) with a value of 1.8 eV to an indirect bandgap of 1.2 eV in bulk [6,7]. The SL semiconductor device exhibits unique optical properties, including strong photoluminescence (PL) [8], valley polarization [9,10] and strongly charged excitons [11].

It is important to note that fabricating MoS_2 electronic devices from mechanically exfoliated flakes is a complex process. In all cases, device size is limited by the geometry of the initial 2D flake, even when a deterministic stamping method is employed [12]. For this reason, tailoring the device after lithographical processing is of interest, regardless of its original geometry. In the past, interacting electron and ion beams have been used with etching gases to pattern different substrates. Reactions of Si, SiO_2 and Si_3N_4 substrates with XeF_2, F_2 and Cl_2 gases were experimentally studied [13]. A similar approach was used with MoS_2 placing it in a XeF_2 atmosphere at high pressure [15]. This process, however, etched the entire exposed surface of the flake, without in situ control of flake geometry. Laser thinning of MoS_2 has been studied [14]. In this case, a control on the flake geometry was reached with size limitation.

In this work our goal is to produce nanostructures in situ, without the need for further lithographical processing. With that in mind, instead of having a two-step post fabrication process consisting of lithography and subsequent etching, (l) the Pulsed Electron-Beam Gas Assisted Patterning (PEBGAP) method combines these two steps into one. This novel nano-patterning method, which uses a carrier gas and an electron beam to laterally etch the channel of an already fabricated MoS2 device into specific geometries. The effect of this fabrication method on the electronic properties of the device will be studied.

---

[1] fernando.jimenez@imdea.org; http://nanoscience.imdea.org/

2. EXPERIMENTAL:

MoS2 flakes were exfoliated onto a degenerately n-doped silicon wafer capped with a 285 nm SiO2 layer. Patterning of electrical contacts is done using laser beam optical lithography, followed by thermal evaporation of chromium (10 nm) and gold (70 nm) resulting in a back-gated field effect transistor geometry. After the contact definition and the liftoff, an annealing is then performed in an argon/hydrogen atmosphere at 300° C to remove resist residues and decrease contact resistance. Electrical transport measurements were carried out in ambient using a probe station and a Keithley 4200 SCS parameter analyzer. Scanning Raman mapping measurements were also carried out in ambient, using a 40x magnification objective, and exciting with a 488 nm Ar laser.

Following the initial characterization of the devices, PEBGAP nano-patterning is used to alter device geometries. This method consists on the combination of a pulsed electron beam and a micro gas injection system. First, the sample is introduced into the Ultra High Resolution Scanning Electron Microscope. Figure 1 shows a schematic view of the process. As shown in Figure 1a, the gas enters the chamber through a small nozzle and adsorbs on the device surface. The eBeam is then pulsed and scanned over the device surface as shown in Figure 1b. The electrons dissociate the gas, causing the fluorine atoms to etch the desired zones of the device, as shown in Figure 1c.
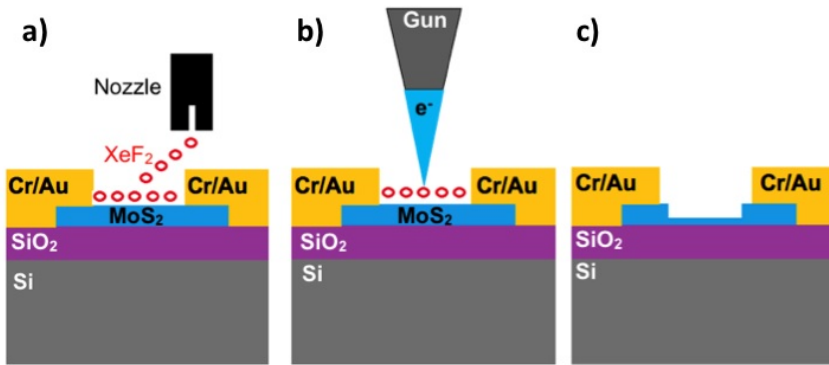

Figure 1. a) Schematic of the gas entering the chamber through the nozzle and adsorbing on the device surface. **b)** Schematic of the focused eBeam scanning the sample. **c)** Final etched device.

After PEBGAP nano-patterning, the devices were characterized again by electrical, AFM and µRaman means. Following this characterization, the devices were annealed at 300 ºC during 2 h and finally characterized.

3. RESULTS:

Figure 2 shows a MoS$_2$ device before and after PEBGAP. Figure 2.a) shows a device width of 2.5 µm. After PEBGAP, a funnel geometry of approximately 250 nm has been created as shown in Figure 2b. A light shadow in the image of Figure 2b, surrounding the funnel device, corresponds to the regions of the original device that were etched. The discoloration is due to a slight etching of the underlying SiO$_2$ substrate, as will be confirmed later in AFM measurements.
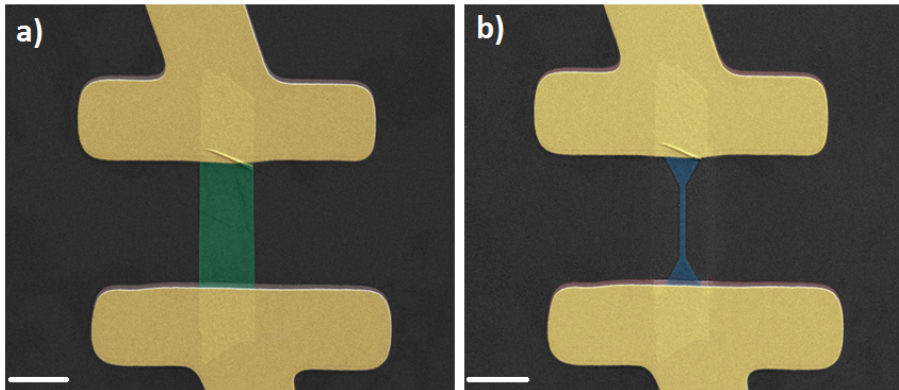
Figure 3a shows an IV curve at 0 back gate voltage before and after PEBGAP. The device was initially 2.5 μm wide and was narrowed to 250 nm. The green IV curve shown in figure 3.a) corresponds to the "intrinsic" device, where a quasi-ohmic contact can be observed. In addition, the blue IV curve in Figure 3a, which corresponds to the device after PEBGAP and annealing, shows a diode-like curve. Apart from the change in curve shape, it also is important to mention that there is a large decrease in the current after PEBGAP. The green curve of Figure 3a is in the μA range, while blue curve is in the nA range. The decrease in channel width after PEBGAP is partially responsible, and should reduce the current to approximately 10% of its initial value.

In addition, doping changes may be playing a role. The transistor curve shown in figure 3.b) reveals that the OFF and ON states of the device before and after PEBGAP are not in the same place. Thus, when measuring at 0 gate voltage, the intrisic device is in the ON state while the PEBGAP device is in the OFF state with values of the current in the nA. A threshold gate voltage shift from -65 V for the intrinsic device to 55 V for the PEBGAP device indicates a p-type doping.
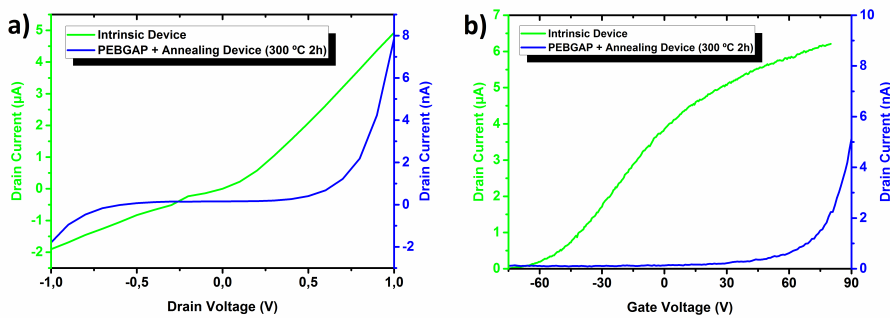

Figure 3. a) IV curve of the intrinsic device (green) and the patterned device (blue). The intrinsic device shows a quasi-ohmic contact while the PEBGAP device shows a diode-type curve. Current scales are different due to two phenomena (narrowing of the channel and changes in doping). **b)** Transistor behavior of the intrinsic device (green curve) and after PEBGAP (blue curve). The ON and OFF states are at different values. A change from -65 V to 55V in threshold voltage after PEBGAP indicates a p-type doping. The saturation of the PEBGAP device cannot be identified due to its doping level.

After PEBGAP processing of the device, bubbles and residues are observed by AFM on the device surface and in the region surrounding it. These could be leftover residues from the etching, particularly on the SiO_2 regions, and XeF_2 gas bubbles trapped within the MoS_2 device. By annealing the device, a much cleaner surface is obtained, as shown in Figure 4b. In addition, a change in device height from 10 to 6 nm is measured before and after annealing. This change in

3

the device height could indicate the disappearance of trapped XeF_2 gas within the MoS_2 layers of the device, and/or the elimination of etching residues between the device and the substrate.. Interaction between the XeF2 gas and the MoS_2 during PEBGAP, or more likely with the trapped gas bubbles during high temperature annealing, could be generating sulfur vacancies within the MoS_2 device channel [REFERENCES HERE?]. Sulfur vacancies are known to have a p-doping effect [OR REFERENCES HERE], as confirmed by experiments using phosphorous plasma immersion ion implantation to create them within a MoS_2 device [20]. This would explain the p-doping observed in the electrical measurements in Figure 3b. Figure 4 also reveals a slight etching of the SiO_2 substrate in the regions where the PEBGAP was carried out, as was previously observed in the SEM images of Figure 2.
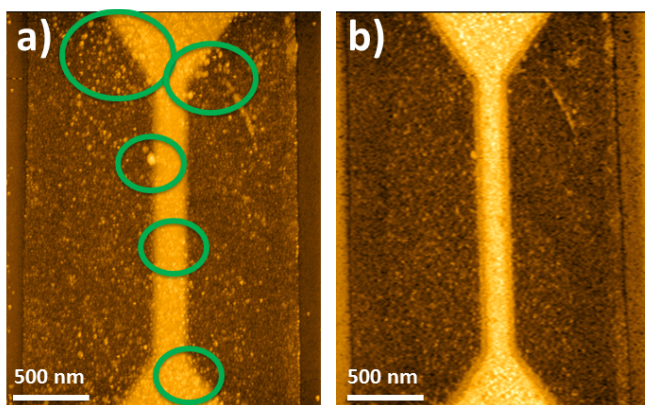

Figure 4. a) AFM image of the processed device before annealing. Green circles round some observed gas bubbles. **b)** AFM image of the processed device after annealing. A decrease in height profile is observed going from 10 nm height before annealing to 6 nm height after annealing.

μRaman characterization of devices before and after PEBGAP give information about structural and chemical composition changes. An intensity mapping of the E^1_{2g} MoS_2 characteristic peak before and after PEBGAP is shown in Figure 5a. The peak's presence after PEBGAP indicates that the post-processing method does not alter the main chemical composition of the MoS_2 device. The A_{1g} peak shows the same behavior as the E^1_{2g} peak, and for that reason only one peak is shown in Figure 5a. Figure 5b shows a full width at half maximum (FWHM) μRaman mapping of the E^1_{2g} peak before and after PEBGAP, revealing a change of the FWHM from 3.5 cm^{-1} before PEBGAP to 5.5-6 cm^{-1} after PEBGAP in the entire flake. The same features are observed for the A_{1g} peak.

Figure 6 represent a μRaman mapping corresponding to the difference in position between the two MoS_2 characteristic peaks (Peak Position Difference, PPD) measured in cm^{-1} before and after PEBGAP, showing a change in the PPD from 23-24 cm^{-1} before PEBGAP to 21-22 cm^{-1} after PEBGAP.

These changes after PEBGAP in FWHM and PPD shown in Figure 5b and Figure 6 respectively could indicate a change in the doping as observed in [24,25], where they attribute changes in μRaman parameters to changes in the doping. Specifically, it was observed an increase in the FWHM and a reduction in the PPD as shown in our results.
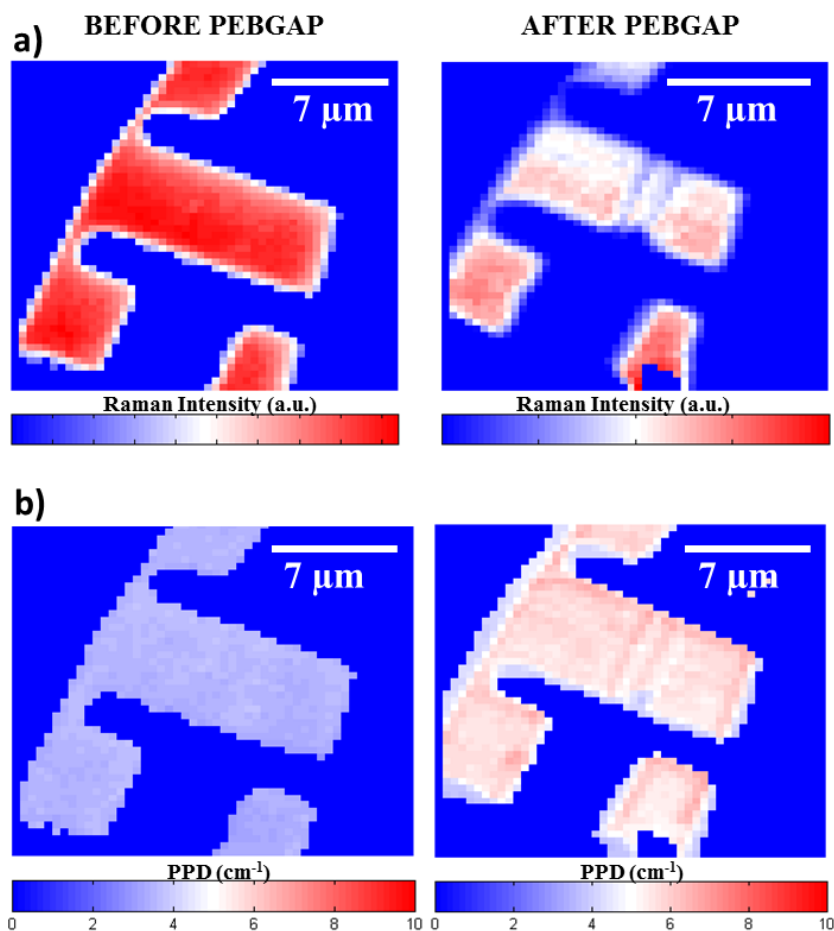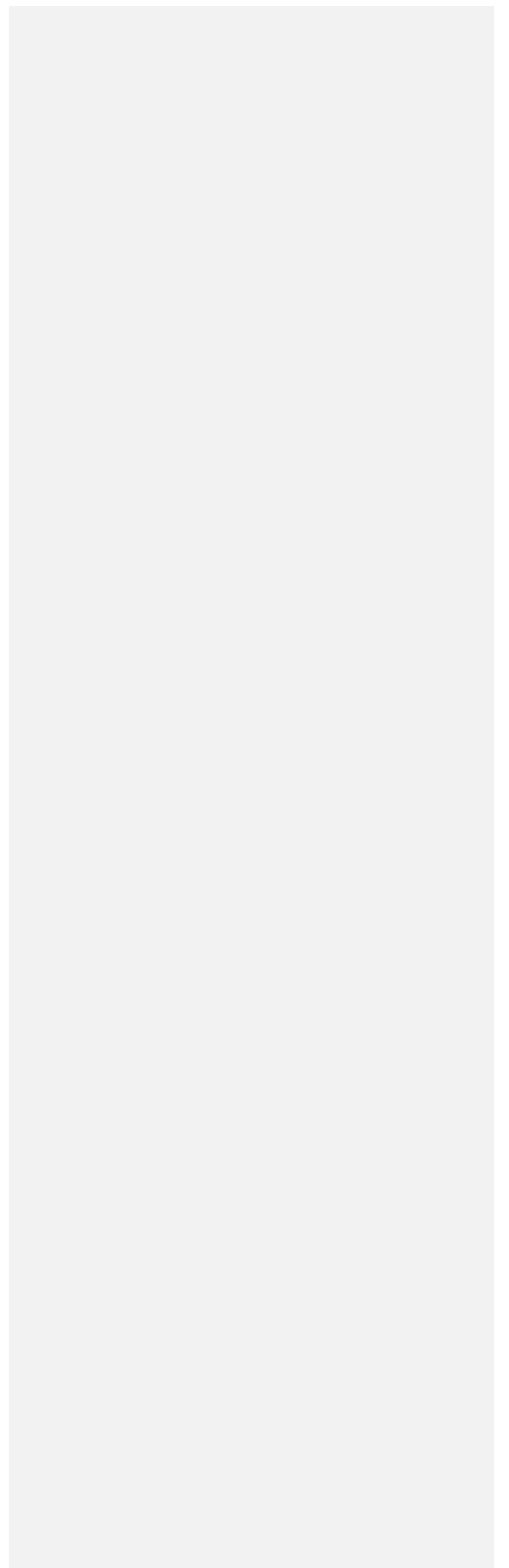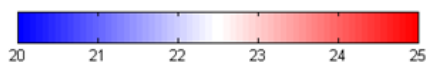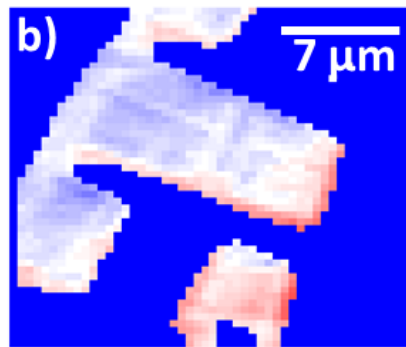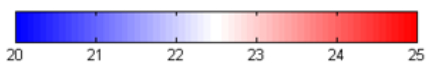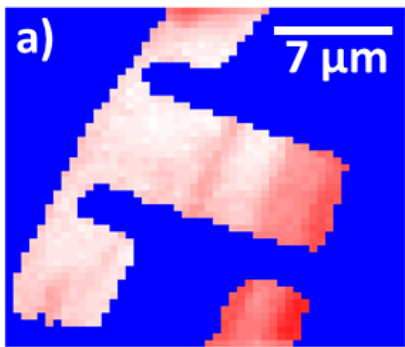
Figure 6. a) μRaman PPD mapping before PEBGAP. PPD value is around 23-24 cm^{-1}. **b)** μRaman PPD mapping after PEBGAP. PPD value is around 21-22 cm^{-1}. A shift to lower values between 2-3 cm^{-1} is observed after PEBGAP indicating, probably, a change in doping.

4. CONCLUSIONS:

The experiments here reported have shown that PEBGAP is a tool that allows tailoring device geometries after fabrication, combining lithographic patterning and subsequent etching into a single step.

After PEBGAP the, device's electrical characteristics are significantly changed,showing a transition from n-type to p-type doping. After PEBGAP, AFM characterization revealed the presence of gas bubbles and etching residues on the device surface and possibly between the layers of the MoS$_2$. These were eliminated by a subsequent high temperature annealing, cleaning the device and the area surrounding it, as well as reducing the height of the device itself. We speculate that the high temperature annealing may cause the MoS$_2$ to interact with the trapped gas and residues, creating sulfur vacancies in the device channel which may be responsible for the observed p-doping, as reported by other authors.

Doping is also revealed by μRaman spectroscopy, which shows a change in the FWHM and PPD values after PEBGAP.

REFERENCES:

[1] Novoselov, K.S. et al. PNAS USA 2005, 102, 10451- 10453

[2] Sina Najmaei et al. ACS Nano 2014, 8, 7930-7937

[3] Xiao Huang et al. Chem. Soc. Rev. 2013, 42, 1934

[4] D.Kufer and G.Konstantanos. Nano Lett. 2015, 15, 7307-7313

6

[5] Jungwook Choi et al. ACS Nano 2016, 10, 1671-1680

[6] Mak, K.F et al. Phys. Rev. Lett. 2010, 105, 136805

[7] Kam, K.K. et al. J. Phys. Chem. 1982, 86, 463-467

[8] Splendiani, A. et al. Nano Lett. 2010, 10, 1271-1275

[9] Mak, K.F. et al. Nat. Nanotechnol. 2012, 7, 494-498

[10] Zeng, H. et al. Nat. Nanotechnol. 2012, 7, 490-493

[11] Ross, J.S. et al. Nat. Commun. 2013, 4, 1474

[12] Castellanos-Gomez, A. et al. 2D Materials 2014, 1, 025001

[13] Coburn, J. et al. Journal of App. Phys. 1979, 50, 3189- 3196

[14] Castellanos-Gomez, A. Nano Lett. 2012, 12, 3187-3192

[15] Huang, Y. et al. Nano Research 2013, 6, 200-207

[16] Hong Li et al. Adv. Funct. Mater. 2012, 22, 1385-1390

[17] Ramon paper PEBGAP

[19] Carvalho, A. et al. Phys. Rev. B: Condens. Matter Mater. Phys. 2014, 89,   081406−081410.

[20] Nipane, A. et al. ACS Nano, 2016, 10, 2128-2137

[21] Dong Min Sim et al. ACS Nano, 2015, 9, 12115-12123

[22] Brahim Akdim et al. Nanotechnology, 2016, 27, 185701

[23] Jinhua Hong et al. Nature Commun. 2015, 520, 656-660

[24] Chakraborty, B. et al. Phys. Rev. B, 2012, 85, 161403

[25] William M. Parkin et al. ACS Nano, 2016, 10, 4134-4142